Emergence of X-Shaped Spatiotemporal Coherence in Optical Waves

O. Jedrkiewicz,[1] A. Picozzi,[2] M. Clerici,[1] D. Faccio,[1] and P. Di Trapani[3]

[1]CNISM and Department of Physics and Mathematics, Università dell'Insubria, Via Valleggio 11, 22100 Como, Italy

[2]Laboratoire de Physique de l'Université de Bourgogne, CNRS UMR 5027, Dijon, France

[3]Department of Quantum Electronics, Vilnius University, Sauletekio 9, LT 01222 Vilnius, Lithuania

(Received 22 July 2006; published 13 December 2006)

Considering the problem of parametric nonlinear interaction, we report the experimental observation of electromagnetic waves characterized by an X-shaped spatiotemporal coherence; i.e., coherence is neither spatial nor temporal, but skewed along specific spatiotemporal trajectories. The application of the usual, purely spatial or temporal, measures of coherence would erroneously lead to the conclusion that the field is fully incoherent. Such hidden coherence has been identified owing to an innovative diagnostic technique based on simultaneous analysis of both the spatial and temporal spectra.

DOI: 10.1103/PhysRevLett.97.243903 PACS numbers: 42.65.Sf, 05.45.−a, 42.25.Kb, 42.50.Ar

Coherence is a key physical concept underlying the statistical properties of a large variety of fundamental phenomena, such as Bose-Einstein condensation, superfluid flows, superconductivity [1,2], laser light emission [3], or hydrodynamic turbulent flows [4]. In optics, which is the natural context to discuss this notion, the simplest manifestations of correlations in fluctuating electromagnetic fields are the well-known interference effects that arise when two light beams originating from the same source are superposed. The elementary concepts of spatial and temporal coherence have been introduced to characterize the statistical properties of partially incoherent optical fields [3]. Spatial coherence refers to the ability of a field to interfere with a spatially shifted (but not delayed) region of the same field, whereas temporal coherence describes the similar ability to interfere with a delayed (but not spatially shifted) version of itself. The mutual coherence function was introduced to provide a unified formulation of the notions of spatial and temporal coherence [3,5,6]. However, despite such a generalized mathematical description of light, common experimental measurements of coherence are usually aimed at providing a separate characterization of the spatial and temporal coherence properties. The coherence time τ_c (e.g., of laser radiation) is conveniently measured by using a Michelson interferometer, while the spatial coherence area ΔA (e.g., of stellar light reaching Earth's surface) may be measured with a Young interferometer [3]. The concept of *coherence volume* around a particular point of the field naturally follows from these definitions as $\Delta V = \Delta l \Delta A$, where $\Delta l = c\tau_c$ is the longitudinal coherence length and c the speed of light [3]. The coherence volume appears then as a space-time factorizable quantity, which corroborates the general idea that a separable characterization of the spatial and temporal properties of coherence provides a convenient description of fluctuating fields, as witnessed by common interferometric measures of coherence. We should remark that to date there has been no experimental direct measurement of a coherence volume over the entire space-time domain.

We report in this work the experimental observation of optical waves characterized by an X-shaped spatiotemporal coherence; i.e., coherence is neither spatial nor temporal, but skewed along specific spatiotemporal trajectories [7]. This reveals that the dichotomous picture of spatial and temporal coherence is not appropriate for the description of the coherence properties of a large variety of nonlinear wave systems. Actually, the nonlinear mechanism underlying the formation of such peculiar coherent states essentially relies on symmetry considerations associated with momentum and energy conservation laws—the phase-matching conditions [8]. This may be illustrated by considering the basic process of degenerate parametric generation, in which a second harmonic (pump) beam, of frequency ω_2, parametrically amplifies the fundamental harmonic signal ($\omega_1 = \omega_2/2$) from quantum noise fluctuations [8,9]. The phase-matching condition projected along the longitudinal axis z of propagation reads $\Delta k_z = k_{2,z}(\omega_2) - k_{1,z}(\omega_1 + \Omega) - k_{1,z}(\omega_1 - \Omega)$, where $\vec{k}_{1,2}$ represent the wave vectors of the beams and Ω a detuning of the signal frequency with respect to ω_1. Expanding the dispersion relation $k_{1,z}(\omega_1 + \Omega)$ to second order in Ω and making use of the paraxial approximation, one readily obtains $\Delta k_z = K^2/k_1 - \Omega^2 k_1''$, where $K^2 = k_{1,x}^2 + k_{1,y}^2$ and $k_1'' = (\partial^2 k_1/\partial\omega^2)$. It becomes apparent that whenever a nonlinear material exhibits normal dispersion $k_1'' > 0$, preferential amplification ($\Delta k_z \simeq 0$) occurs for spatial and temporal frequencies lying along an X-shaped spectrum, defined by two symmetric lines $K = \pm\sqrt{k_1 k_1''}\Omega$ (see Fig. 1). This intriguing spectrum will be shown to witness the presence of a field featuring an X-shaped correlation function in the space-time domain, i.e., a coherence volume characterized by a nonfactorizable, spatiotemporal, biconical (hourglass) shape. Owing to an innovative experimental technique, we provide a direct characterization of such a nontrivial volume of coherence. To our knowledge, this constitutes the first measurement of correlations over the entire space-time domain.

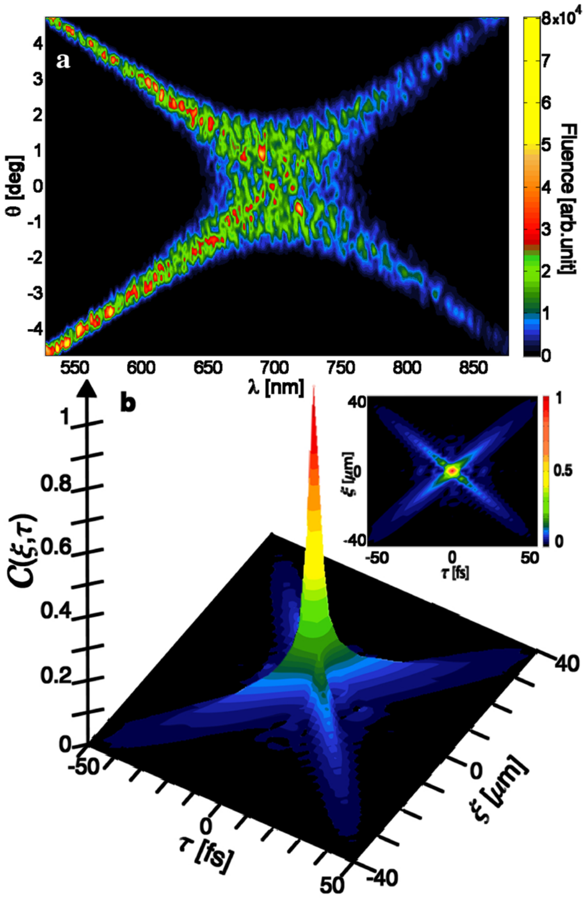

FIG. 1 (color online). (a) Spatiotemporal spectrum $\mathcal{S}$ of the signal field generated from amplification of the quantum fluctuations by a single pump pulse. (b) X-shaped spatiotemporal correlation function $\mathcal{C}(\xi, \tau)$ of the signal field calculated from the Fourier transform of the averaged spectrum $\langle \mathcal{S} \rangle$. The inset shows the contour-plot representation of (b).

This novel state of X coherence is shown to emerge from the combined action of (spatial) diffraction, (temporal) dispersion, and nonlinearity. In this respect, the generation process represents the stochastic counterpart of the deterministic formation of nonlinear X waves, which are coherent localized structures recently discovered in various contexts [9–11]. The concept of X coherence may become of central importance for the study of spatiotemporal delocalization properties inherent to quantum objects.

The experiment is conceptually simple. It relies on a much used experimental configuration of parametric superfluorescence generation in a quadratic, $\chi^{(2)}$, nonlinear crystal [8]. The pump pulse is given by a $T_p = 1$ ps duration, $\Delta\lambda_p = 0.1$ nm spectral bandwidth (centered at $\lambda_2 = 352$ nm), $D_p = 200$ μm diameter, $E_p = 80$ μJ energy (peak power $P = 80$ MW), transform-limited Gaussian pulse. It is generated by frequency tripling the output of a chirped pulse amplification Nd:glass laser, operated at a 2 Hz repetition rate. The pump pulse is injected into a 2-mm-long beta barium borate (BBO) crystal, cut for a type I degenerate interaction at $\lambda_1 = 704$ nm. As a result of the parametric generation process, the spatiotemporal dimensions of the signal beam are of the same order than those of the pump, a feature confirmed by our measurements. The spectrum $\mathcal{S}(\theta, \lambda)$ of the generated signal is analyzed in both the spatial and temporal domains; i.e., it is resolved in vertical angle $\theta \simeq K/k_1$ and in wavelength λ ($\omega_1 + \Omega = 2\pi c/\lambda$). For this purpose, the entrance slit of an imaging spectrometer (Oriel Instruments, MS260i) is placed in the focal plane of a $f = 75$ mm focusing lens that collects the signal radiation. This setting allows different vertical-angle components of the impinging radiation to enter the slit at different vertical positions. The spectrum $\mathcal{S}(\theta, \lambda)$ is acquired by a high dynamic-range (16-bit) CCD camera (Andor, EEV 40-11), placed in the spectrometer imaging plane, and a laser-synchronized shutter permits single-shot acquisition of the radiation generated by a single laser pulse.

Figure 1(a) illustrates a typical example of spatiotemporal signal spectrum $\mathcal{S}$ retrieved from a single pump pulse. It exhibits an X-shaped structure, which indicates the emission of radiation at angles θ increasing with the frequency shift Ω, as previously anticipated by the linear relationship $K = \pm\sqrt{k_1 k_1''}\Omega$. Such X spectra are known to characterize X waves [9–11], which constitute the polychromatic generalization of diffraction-free Bessel beams [12]. However, in contrast to X waves, which are inherently coherent localized structures (i.e., characterized by smooth X spectra [11]), here the spectrum exhibits a specklelike substructure reflecting the (partially) incoherent nature of the field [13]. The signal field may thus be considered as a random superposition of uncorrelated X-like waves. Note that the spectrum is extended over very large temporal and spatial bandwidths, ΔK and $\Delta\Omega$ ($\Delta\Omega$ almost spans the complete visible spectrum). If the radiation were analyzed by means of traditional techniques, one would be led to the erroneous conclusion that the field is spatially and temporally almost incoherent, since $\tau_c \sim 2\pi/\Delta\Omega \sim 5$ fs and $\Delta l \sim 2\pi/\Delta K \sim 3.5$ μm. However, in contrast to usual incoherent fields, whose spectra uniformly fill the space-time frequency domain (K, Ω), here the spectrum is sharply localized over a thin X-shaped surface. The coherence hidden in this peculiar spectrum is revealed through the analysis of the spatiotemporal correlation function $\mathcal{C}(\xi, \tau)$. $\mathcal{C}(\xi, \tau)$ is calculated from the Fourier transform of the averaged spectrum $\langle \mathcal{S}(K, \Omega) \rangle$ by making use of the generalized form of the Wiener-Kintchine theorem [13]. The average over realizations $\langle \mathcal{S}(K, \Omega) \rangle$ is recorded from multiple-shot on chip integration by keeping the shutter open for a suitable time interval. Note that in computing the average, the dependence on the vertical detection plane is removed owing to the radial symmetry with respect to the z axis. As revealed by Fig. 1(b), $\mathcal{C}(\tau, \xi)$ also turns out to be X shaped [Fig. 1(b)], indicating that two points in the field are correlated with each other only if their temporal delay τ and spatial distance ξ belong to such an X structure. Because of the radial symmetry of the system, $\mathcal{C}$

depends only on the modulus $|\vec{\xi}|$, so that the X-shaped correlation function corresponds to a biconical shape in three dimensions [13].

Further insight into X coherence may be gained by analysis of Maxwell's equations describing the propagation of the optical fields in the crystal [8]. In the parametric regime of amplification the signal envelope is known to satisfy $\{\partial_{zz} + 2ik_1\partial_z + [k^2(\omega_1 + \Omega) - k_1^2 - K^2]\}\hat{A}_1(\vec{K}, \Omega) = -\sigma\hat{A}_1^*(-\vec{K}, -\Omega)$, $\sigma = \chi^{(2)}\omega_1^2 P^{1/2}/2c^2$. The analytic expression for the growth rate $\gamma(K, \Omega)$ of the parametric amplification process is extremely involved in the general case. It is worth noting, however, that the angular-spectrum of the radiation is relatively narrowband [$\Delta\theta \simeq 5^0 = 0.09\text{Rd} \ll 1$ in Fig. 1(a)], so that physical insight may be obtained in the limit of the paraxial approximation,

$$\gamma(K, \Omega) = i\mathcal{I} + \sqrt{\sigma^2/4k_1^2 - (\mathcal{P} - K^2/2k_1)^2}, \quad (1)$$

where $\mathcal{I} = \sum_{i=0}^{\infty} \Omega^{2i+1} k_{\omega_1}^{(2i+1)}/(2i+1)!$ and $\mathcal{P} = \sum_{i=1}^{\infty} \Omega^{2i} k_{\omega_1}^{(2i)}/(2i)!$ refer to the odd and even expansions of $k(\omega_1 + \Omega) = \mathcal{P} + \mathcal{I}$. The evolution of the signal envelope is found to be $\hat{A}_1(\vec{K}, \Omega, z) = U(\vec{K}, \Omega)\hat{A}_1(\vec{K}, \Omega, 0) + V(\vec{K}, \Omega)\hat{A}_1^*(-\vec{K}, -\Omega, 0)$, where $U(\vec{K}, \Omega) = \exp(i\mathcal{I}z) \times [\cosh(\Gamma z) + i\frac{\Delta}{\Gamma}\sinh(\Gamma z)]$ and $V(\vec{K}, \Omega) = \exp(i\mathcal{I}z)\frac{i\sigma}{2k_1\Gamma} \times \sinh(\Gamma z)$, with $\Delta = \mathcal{P} - K^2/2k_1$, $\Gamma = (\sigma^2/4k_1^2 - \Delta^2)^{1/2}$. Note that this solution is valid beyond the usual slowly varying envelope approximation [8]. In the limit of large propagation distances, the spectrum may be approximated by $\langle \mathcal{S}(K, \Omega, z)\rangle = \langle|\hat{A}_1|^2\rangle \propto \exp[2\gamma_r(K, \Omega)z]$, where $\gamma_r = \text{Re}(\gamma)$. Within the slowly varying envelope approximation, the growth rate reduces to $\gamma_r = [\sigma^2/4k_1^2 - (k_1''\Omega^2/2 - K^2/2k_1)^2]^{1/2}$. It becomes apparent that, in contrast to the anomalous dispersion regime ($k_1'' < 0$), where $\gamma_r(K, \Omega)$ has a symmetric structure reflecting the symmetric role of space and time, in normal dispersion ($k_1'' > 0$) $\gamma_r(K, \Omega)$ exhibits a hyperbolic structure; i.e., the locus $(K - \Omega)$ of the peak gain is X shaped, as previously anticipated. The evolution of the correlation function $\mathcal{C}(\tau, \xi, z)$ shows a progressive emergence of X coherence reminiscent of the growth of starfish arms (see Fig. 2). Accordingly, the signal field becomes self-correlated along two specific spatiotemporal trajectories, $\tau = \pm\sqrt{k_1 k_1''}\xi$, as confirmed by the numerical simulations [Fig. 2(b)]. Let us remark that, in the limit in which dispersion (diffraction) dominates the interaction, i.e., when k_1'' tends to infinity (zero), the arms of the X-correlation function become superposed and parallel to the temporal (spatial) axis. It is only in these two particular cases that the coherence properties of the generated field can be correctly described by the usual concepts of spatial or temporal coherence.

The existence of X coherence is corroborated by an interferometric measurement based on the celebrated Young's two-pinhole experiment [7]. Rather than producing the usual single-peak fringe pattern [3], X coherence is shown to lead to a double-peak pattern (Fig. 3), where each peak arises from one arm of the X correlation. Indeed, the fringe visibility is given by the normalized correlation function $\mathcal{C}(\xi = a, \tau)$, in which ξ is fixed to the distance a ($= 30\ \mu$m) between the pinholes and τ corresponds to the time delay between the two beams coming from the two pinholes [3]. The double-peak structure then reflects the ability of the field to interfere with a spatially shifted version of itself, provided it is delayed by appropriate times $\tau_\pm$, determined by the spatiotemporal trajectories $\tau_\pm \simeq \pm\sqrt{k_1 k_1''}a$. The limited visibility of the fringes in Fig. 3 may be ascribed to the short time correlation ($\tau_c \simeq 5$ fs), which is close to the optical cycle time and thus limits the spatial extension of the visibility pattern Δx to the fringe period i_0 ($\Delta x/i_0 = c\tau_c/\lambda_1 \simeq 1$).

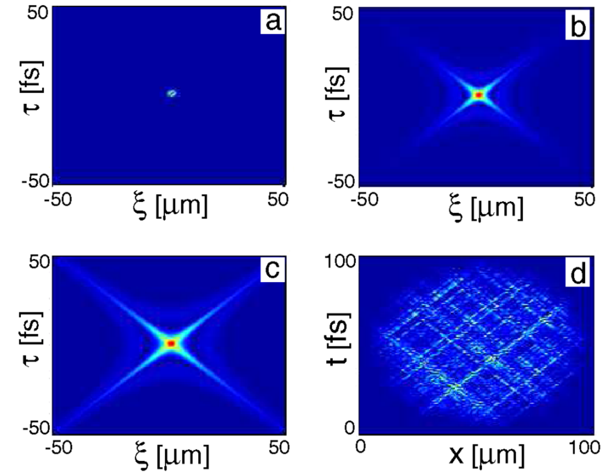

FIG. 2 (color online). Theoretical evolution of the spatiotemporal correlation function $\mathcal{C}(\xi, \tau, z)$ during the propagation of the signal field in the crystal, $z = 0$ (a), $z = 1$ mm (b), and $z = 2$ mm (c). (d) Numerical simulation showing the spatiotemporal intensity distribution of the signal field at propagation distance $z = 2$ mm [the simulation has been performed in (2 + 1) dimension, in the paraxial and slowly varying envelope approximation].

Let us stress the general relevance of X coherence by underlining that it constitutes the natural state of coherence for all nonlinear systems whose governing equations exhibit a space-time hyperbolic structure, as discussed above through Eq. (1). X coherence is thus expected to arise in any multidimensional optical system involving nonlinear wave propagation in normal dispersion. A typical example is the modulational instability of plane waves propagating in cubic, $\chi^{(3)}$, nonlinear Kerr media [14]. In complete analogy with the present work, we have verified that X coherence emerges spontaneously in Kerr media in the modulational amplified noise fluctuations (data not shown). Note that space-time skewed coherence does not necessarily require radial symmetry in the phase-matching configuration; it is indeed sufficient to consider a noncollinear, planar interaction geometry. Consider, e.g., the

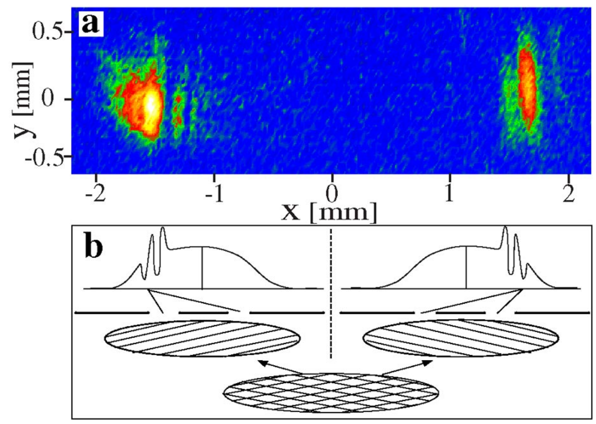

FIG. 3 (color online). (a) Experimental fringe pattern obtained by means of Young's interference experiment. The signal radiation is recorded using a CCD camera placed 23 mm behind the two-pinhole screen. (b) Schematic representation of Young's interference experiment explaining the origin of the double-peak structure of the visibility pattern: The condition for interference between two regions of the field requires an appropriate shift in both space and time so that the peak-visibility results to be shifted to the two points where such condition is satisfied. Each peak then corresponds to one arm of the X-correlation function of Fig. 1(b).

standard process of four-wave mixing supported by a cubic nonlinearity, in which two noncollinear pump waves parametrically amplify two daughter waves from noise fluctuations [8]. In this case, coherence emerges along those skewed spatiotemporal trajectories where spatial walk-off and temporal group-velocity difference compensate each other [7], in the same way that X coherence emerges along skewed lines where diffraction compensates chromatic dispersion. Four-wave mixing is indeed a very general process; it is known to play a key role not only in optics, but also in such diverse fields as plasma [15], acoustic [16], water [17], and matter waves [2]. Considering specifically the process of parametric four-wave mixing in Bose-Einstein condensates [2], we may reasonably infer the formation of long-range phase coherence (condensation) along specific spatiotemporal lines. This feature might be revealed by means of (Young's) double-slit interference experiments [18]. However, following the spectral technique reported here, an alternative approach would consist in detecting correlation directly in the momentum distribution (spectrum) of the expanded matter wave.

Finally, we point out the natural importance that X coherence may have in the context of quantum optics. Referring again to the parametric generation process, one may reasonably expect that the X-shaped spectrum [Fig. 1(a)], as well as the double-peak fringe pattern (Fig. 3), would be similarly obtained if the acquisition were performed in the parametric fluorescence regime, i.e., photon by photon. This implies that each individual photon would be characterized by an X-shaped space-time correlation.

P. D. T. acknowledges the EU Marie Curie Chair action "STELLA," MEXC-2005-025710.

[1] J. F. Annett, *Superconductivity, Superfluids and Condensates* (Oxford University Press, New York, 2004).
[2] P. Meystre, *Atom Optics* (Springer-Verlag, New York, 2001).
[3] L. Mandel and E. Wolf, *Optical Coherence and Quantum Optics* (Cambridge University Press, New York, 1995); J. W. Goodman, *Statistical Optics* (Wiley-Interscience, New York, 1985).
[4] U. Frisch, *Turbulence: The Legacy of A. N. Kolmogorov* (Cambridge University Press, New York, 1995).
[5] E. Wolf, Proc. R. Soc. A **230**, 246 (1955).
[6] L.-G. Wang *et al.*, Phys. Rev. E **67**, 056613 (2003).
[7] A. Picozzi and M. Haelterman, Phys. Rev. Lett. **88**, 083901 (2002).
[8] R. W. Boyd, *Nonlinear Optics* (Academic Press, New York, 2002).
[9] S. Orlov *et al.*, Opt. Lett. **27**, 2103 (2002); R. Butkus *et al.*, Opt. Commun. **244**, 411 (2005); S. Trillo *et al.*, Opt. Lett. **27**, 1451 (2002).
[10] C. Conti *et al.*, Phys. Rev. Lett. **90**, 170406 (2003); P. Di Trapani *et al.*, Phys. Rev. Lett. **91**, 093904 (2003); M. Kolesik *et al.*, Phys. Rev. Lett. **92**, 253901 (2004); D. Faccio *et al.*, Phys. Rev. Lett. **96**, 193901 (2006); C. Conti and S. Trillo, Phys. Rev. Lett. **92**, 120404 (2004).
[11] D. Faccio *et al.*, J. Opt. Soc. Am. B **22**, 862 (2005).
[12] J. Durnin, Jr. Miceli, Jr., and J. H. Eberly, Phys. Rev. Lett. **58**, 1499 (1987).
[13] Given the short signal pulse duration, the statistics of the signal field cannot be assumed to be stationary. The correlation function $\mathcal{R} = \langle A_1(\vec{r}_1, t_1, z) A_1^*(\vec{r}_2, t_2, z)\rangle$ is thus given by means of the generalized form of the Wiener-Kintchine theorem, $\mathcal{R}(\tau, \vec{\xi}, t, \vec{r}, z) = \int d\tau \int d\vec{\xi} \int dt \int d\vec{r}\, \hat{\mathcal{R}}(\Omega, \vec{K}, \omega, \vec{k}, z) \exp[i(\Omega\tau + \vec{K}\cdot\vec{\xi} + \omega t + \vec{k}\cdot\vec{r})]$, where $\hat{\mathcal{R}} = \langle \hat{A}_1(\vec{K}_1, \Omega_1, z)\hat{A}_1^*(\vec{K}_2, \Omega_2, z)\rangle$, $\tau = t_1 - t_2$, $\vec{\xi} = \vec{r}_1 - \vec{r}_2$, $t = \frac{1}{2}(t_1 + t_2)$, $\vec{r} = \frac{1}{2}(\vec{r}_1 + \vec{r}_2)$, $\Omega = \frac{1}{2}(\Omega_1 + \Omega_2)$, $\vec{K} = \frac{1}{2}(\vec{K}_1 + \vec{K}_2)$, $\omega = \Omega_1 - \Omega_2$, $\vec{k} = \vec{K}_1 - \vec{K}_2$, and $\vec{r} = (x, y)$. However, the typical size of the speckles reported in the experiment, $\delta\omega \sim T_p^{-1}$, $\delta k \sim D_p^{-1}$, is much smaller than the size of the X spectrum [Fig. 1(a)]. $\hat{\mathcal{R}}$ may thus be factored as $\hat{\mathcal{R}} \simeq \langle \mathcal{S}(\vec{K}, \Omega, z)\rangle \hat{I}(\vec{k}, \omega, z)$, where $\hat{I}$ takes into account the nonstationarity of the signal statistics through the finite size of the speckles. The function $\mathcal{R} = \mathcal{C}(\vec{\xi}, \tau, z) I(\vec{r}, t, z)$ turns out to be the product of a stationary contribution $\mathcal{C}(\vec{\xi}, \tau, z)$, and a nonstationary contribution $I(\vec{r}, t, z)$, i.e., the space-time intensity profile of the signal pulse.
[14] L. W. Liou *et al.*, Phys. Rev. A **46**, 4202 (1992); G. G. Luther *et al.*, Opt. Lett. **19**, 789 (1994).
[15] J. Weiland and H. Wilhelmsson, *Coherent Nonlinear Interaction of Waves in Plasmas* (Pergamon, Oxford, 1977).
[16] M. F Hamilton and D. T. Blackstock, *Nonlinear Acoustics* (Academic Press, New York, 1998), Chaps. 8 and 14.
[17] E. Infeld and G. Rowlands, *Nonlinear Waves, Solitons and Chaos* (Cambridge University Press, Cambridge, England, 1992).
[18] I. Bloch *et al.*, Nature (London) **403**, 166 (2000).